Pavement FRFs and noise: A theoretical and experimental investigation

Pavement FRFs and noise: a theoretical and experimental investigation

Filippo G. Praticò, Rosario Fedele and Gianfranco Pellicano

DIIES Department, Mediterranea University of Reggio Calabria, Italy

Abstract

Traffic and tyre/road noise affect human health. In order to mitigate the tyre/road noise, the knowledge of the frequency-based mechanics of pavements (e.g., pavement Frequency Response Functions, FRF) could be a crucial factor, because the remaining factors have been investigated in depth.

Consequently, the main objective of this study was to investigate the relationships between road acoustic response (herein called RAR) and FRFs in case of bituminous mixtures added with different percentages of crumb rubber (CR).

Laboratory tests and analyses were carried out. In particular, during preliminary tests, the system (i.e., impact hammer, microphone, analog-to-digital converter cards, and software) was set up using both cylindrical specimens and rectangular slabs, and a new testing procedure for both sample types (based on the standards EN29052-1 and ISO 7626-5) was defined.

Subsequently, the new procedure was applied to four sets of cylindrical samples consisting of dense asphalt concretes (i.e., AC6d), where different percentages of crumb rubber (CR; i.e., 5 %, 29 %, and 100 %) were added (dry method).

Results demonstrate that even if many parameters affect the FRF estimates, FRFs and RAR are related especially in the range 0.4-3.2 kHz, and that CR content can contribute to lowering the mechanical impedance, the dynamic stiffness, and the acoustic response of the asphalt concrete mixtures used in this study.

By referring to RAR-based versus Close Proximity method (CPX)-based inferences and analogies, the relationship between the RAR herein defined and measured and the on-road CPX emerges as mainly unknown and probably quite complex.

Further investigations are required to have a higher accuracy of the results and to better understand CR actual impact on tyre/road noise and remaining properties.

Keywords: Frequency Response Function, Mechanical Impedance, Dynamic Stiffness, Tyre/Road Noise, Impact Hammer, Crumb Rubber.

1. Introduction

Traffic noise represents one of the most important factors that influences urban noise. In big cities and main access roads, traffic noise level may exceed the thresholds of healthy exposure [1]. Noise can cause sleep disturbances, cardiovascular and psychophysiological diseases, changes in social behaviour [2], and live losses [3]. Traffic noise and vibrations impact urban liveability [4–6], the environment [7], and indirectly the service life and costs of pavements (maintenance and rehabilitation, cf. [6]).

Traffic noise depends on the power unit of the vehicles (especially for speeds lower than 40 km/h) and on tyre-road contact (tyre/road noise, especially for speed higher than 30-50 km/h) [8]. In turn, tyre/road noise includes aerodynamic effects and vibratory phenomena (see e.g., [9]) and mainly depends on tyre properties (e.g., tread design) and pavement properties, such as macrotexture, friction between tyre and road surface, and the frequency response of the road to a mechanical load [10].

In the last decades, different strategies have been proposed to reduce the effects of traffic noise, and the following section summarizes the noteworthy ones.

In this study authors focused the attention on the relationships between Road Acoustic Response (RAR) and FRFs in case of bituminous mixtures with the addiction of crumb rubber (CR), where FRFs (a.k.a. transfer functions) can be defined as "the frequency domain relationship between an input (X) and output (Y) of a linear, time-invariant system" [11]. Examples of FRFs are the Mechanical Impedance (*MI*, i.e., the ratio between the

force applied on a body, *X*, and the velocity of the body excited by the force, *Y*), and the Dynamic Stiffness (*K*, i.e., the ratio between the force applied on a body, *X*, and the displacement of the body excited by the force, *Y*).

2. Literature review

Based on relevant European guidelines [12,13], the aforementioned strategies may be grouped as follows: 1) Reduction acting on the source (i.e., vehicles, tyre/road interaction, speed, and traffic density). 2) Reduction acting on the receiver (e.g., through noise barriers, sound-proof windows, urban planning and providing an appropriate distance between road and receiver where possible).

The study described in this paper deals with asphalt concrete composition, as a means to affect tyre-road interaction. Note that many studies and projects were carried out.

Sandberg and Ejsmont [14] provided a general and comprehensive overview for the interested environmental experts in the field of tyre/road noise.

During the European project ROADTIRE [15] other international projects related to the acoustic performance of low-noise pavements (i.e., bituminous mixtures incorporating tyre rubber particles) have been studied and a noise level reduction between 2 to 10 dB (with the A-weighing filter applied) was observed.

Vaitkus et al. [16,17] presented laboratory studies that aimed at optimizing the noise reducing properties of traditional Stone Mastic Asphalt (SMA 5 and 8), Asphalt Concrete (AC 5), and Porous Asphalt (PA 8) mixtures, and reported an expected noise reduction of 2-5 dB compared to the mixtures (SMA 8, SMA 11 and AC 11) used traditionally in Lithuania.

Usually, the Close Proximity (CPX) method is used to assess the tyre-road noise [18], and two main aspects should be considered when low-noise road pavements are used, i.e. the durability and the acoustic aging (mainly due to clogging and raveling).

Mioduszewski and Gardziejczyk [19] presented a study related to the EU project ROSANNE, in which they compared the A-weighted sound pressure level (SPL) of PA 8, a very thin AC (BBTM 8), SMA 5 and SMA 11. They found three main causes of low-noise pavement inhomogeneity, namely, imperfections in the technology used for asphalt mix production, clogging, and excessive wear of the pavement (raveling).

Vuye et al. [20] applied the CPX and the Statistical Pass-By (SPB) methods to a noise-reducing Thin Asphalt Layer (TAL, maximum thickness of 30 mm, and air void content, AV, of 18 %). They compared the results to those of a double-layer PA and a SMA 10. The TAL showed an initial noise reduction of about 6 dB, but deterioration phenomena led, after 3 years, to a reduction of about 1 dB only.

A comparative study was presented by Bendtsen et al. [21] to evaluate the acoustic aging of Californian and Danish asphalt pavements including Dense-Graded Asphalt Concretes (DGAC), Open-Graded Asphalt Concretes (OGAC), Thin Open-Graded Asphalt Concrete (TOGAC), and PA mixtures. The study highlighted that: 1) The relationship between pavement age and noise level can be well represented by using linear regression models for both passenger cars and multi axle heavy vehicles. 2) The highest noise increase *per* year was obtained for the TOGAC mixes (0.84 dB, passenger cars), followed by PAs (0.53 dB), OGACs (0.41 dB), and DGACs (0.4 dB).

Kragh et al. [22] presented a report of the Danish DRI-DWW noise abatement program, in which road pavements built using different dense graded ACs (AC6d, 8d, 11d and 16d), open graded ACs (AC6o, 8o and 11o), open graded Soft Asphalts (SA6o), SMAs (SMA 6, 8 and 11), BBTMs (BBTM 6, 8 and 11), Double-Layer PAs (DLPA 5/16, 5/22 and 8/16), and Surface Dressing (SD 2/5, 5/8 and 5/8+8/11) mixtures were tested, applying the CPX method (an Hot Mix Asphalt, HMA, 11/16 was used as a reference). At 50 km/h, newly laid ACs and SMAs showed a CPX level of 90 dB, BBTMs of 89-92 dB, PAs of 88 dB and SD of 91-92 dB. Note that an increase of only 1 dB was recorded, after 6-9 years, for AC8 and AC11 and an overall increase of 1-2

dB was observed for Nominal Maximum Aggregate Size (NMAS) from 8 mm to 11 mm. The CPX measurements were repeated, at 50 km/h, after 15 months, obtaining CPX levels of about 89 dB (for AC6o), 91.5 dB (AC11d), 88-92.5 dB (BBTMs), 87-88.5 dB (DLPAs), and of about 89-91 dB (SMAs). Finally, BBTM6 and AC6o yielded the lowest values of SPB levels for passenger cars at low speeds, although an increase of 1.6 dB was observed for the BBTM 6 mix after 1 year from.

A plenitude of studies was carried out aiming at developing more performing and more sustainable asphalt binder/mixtures acting both on mixture composition and production. In particular, the possibility to use the rubber recycled from scrap tyres (Crumb Rubber, CR) was deeply investigated [23–26].

Losa et al. [27] focused on rubberised mixes (wet method) and their noise performance and there is a growing interest in the theoretical and experimental aspects related to the dynamic response and frequency-based response of pavement structures. Teti et al. [28] presented a new method to model CPX broadband levels of newly laid and low-noise road surfaces based on their main parameters (e.g., grading curve, fractal dimension, asphalt binder content, air voids, and voids in mineral aggregates).

Donavan and Janello [29] wrote a report containing the results of the 10 years Arizona quiet pavement pilot program that aimed at evaluating (using the OBSI method, residential neighbourhood noise measurement, and direct traffic-noise measurements) the noise benefit of asphalt rubber friction courses used for urban freeways. An initial reduction in the range 5.2-9.1 dB and an average increase of 0.5 dB/year were observed.

Licitra et al. [30] provided a model for the estimation of the acoustic ageing of rubberized pavements.

Environmental benefits, such as carbon emission reduction and resource conservation (raw material and energy), can be obtained [31] if CR is used to modify the bitumen (wet process) or as a part of aggregates (dry process). Wang et al. [32] studied the application of the Warm Mix Asphalt (WMA) technology on rubberized asphalt mixtures, and concluded that: 1) This type of mixture allows saving approximately 20-25 % of fuel with respect to the Hot-Mix Asphalt (HMA) technology for the aforementioned mixtures. 2) The emissions of O_2, N_2, CO_2, NO_x and SO_2 in the production of rubberized asphalts are somewhat similar to the ones for HMAs (ranging from +0.5 to -10.7 %). 3) During production and construction of rubberized asphalts, the emissions of CO and CH_4 are lower than those produced for HMAs (-39.7 % for CO and -61.7 % for CH_4). 4) For rubberized asphalts, about 40-88 % of tyre/road noise in the frequency range of 500-4000 Hz can be reduced compared to traditional bituminous mixtures. 5) LCA-related results show that the difference between HMAs and WMAs, expressed in terms of energy (related to construction, maintenance and operation processes) is about 37.5 GJ/Km/year.

Note that Poroelastic Road Surfaces (PERS) are an example of mixture containing CR. In the project PERSUADE [33–35] (CR percentage of 32-50 %, dry process), they showed an initial noise reduction in the range 7.6-12.1 dB. Furthermore, a considerable effort was put forth to characterise the dynamic response (mechanical impedance and stiffness) of the aforementioned PERS [33–35], aiming at investigating the noise that refers to tyre vibrations. Li et al. [36,37] studied the mechanical impedance of different pavements through tests carried out in the laboratory or *in situ*.

Thence, it seems relevant to highlight that the hardness of the road surface (and its FRFs) could affect 1) Tyre vibration and consequent noise (structure-borne sound in the tyre, cf. [16]). 2) The transmission of power from the tyre to the pavement and consequently the possible sound radiation from the road. 3) The dependency of such phenomena on the natural frequency of the road (especially for bridge decks).

3. Objectives and study outline

Based on the analysis of the literature, it appears that unfortunately the relationship between tyre/road noise and the frequency response of the pavement is still mainly unknown. The complexity of such an assessment is increased by the fact that mixture composition can affect at the same time surface-, volumetric-related properties [38], and dynamic response and this makes it difficult to split their contribution.

Consequently, the main objective of this study is to investigate the relationships between road acoustic response (herein called RAR) and FRFs for bituminous mixtures added with crumb rubber (CR).

In order to pursue the objective mentioned above, the study was organized in the following tasks:

Task 1: Analysis of literature and standards about Frequency Response Functions (including algorithms, standards, and results in the literature).

Task 2.1: Measurement system set up.

Task 2.2: Preliminary tests and discussion. Experiments on different materials were carried out, using the measurement system cited above (Task 2.1), to set up the test methodology investigating on the influence of the main boundary conditions under which cylindrical samples or slabs are tested (i.e., load plate diameter, gypsum cylinders or not, type of under-layer). Results were discussed and used for interpreting the results of the next task. Tasks 2.1 and 2.2 are reported in section 5 below.

Task 3: Tests on CR-added mixes, applying the methodology defined in the subsection above (where CR stands for crumb rubber). Following the experiments, results were discussed in order to derive consequences and conclusions (Task 4). This task is referred to in sections 6 and 7 below.

Task 3.1: Mixture design and sample production (a specific reference mixture was selected and new mixtures containing different percentage of CR were produced).

Task 3.2: Tests and result analysis.

Task 4: Conclusions (section 8 below).

The tasks listed above and the rationale behind are illustrated in Figure 1.

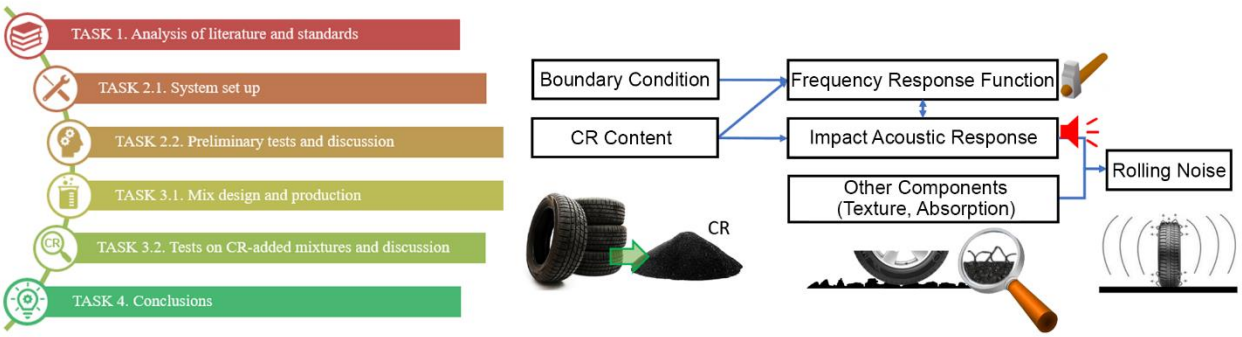

Fig. 1. Tasks performed and rationale behind

Note. No acoustical measurements of "rolling noise" were carried out.

Consequently, the remaining parts of the paper are organized as follows. The next section (section 4) focuses on frequency response functions, while the successive one (section 5) focuses on Task 2. Section 6 explains the design of the mixtures used to produce the samples that have been tested in the experimental investigation (section 7). Section 8 contains the conclusions.

4. Application of FRFs in literature and standards

This task focuses on the analysis of literature and standards about Frequency Response Functions (FRFs).

FRFs give insights into a structure's resonant frequencies (e.g., peaks or dips), damping (width of the peaks), and mode shapes [39]. Many types of input excitations and response outputs can be used to calculate an experimental FRF, based on the system under analysis, e.g., acoustical systems, combined acoustic and mechanical systems, rotational mechanical systems, or mechanical systems, with inputs in force (N) and outputs in acceleration (m/s^2), velocity (m/s), or displacement (m).

FRF format depends on the particular study and different math operations may be applied (e.g., integration and differentiation, inversion). Being these applications in the frequency domain, integration and differentiation correspond to division and multiplication by $j\omega$, respectively, where ω is the frequency in radians per second and j is the imaginary number [39].

The following FRF-related standards can be listed: EN 29052-1 [40], ISO 7626-5 [41], ASTM C125 [42], and EN 14146 [43,44]. These standards regulate how to derive (1) the mechanical impedance of structures, (2) the dynamic stiffness of square slabs used for floating floors, (3) the mechanical mobility and other frequency-response functions of structures excited by means of impulsive forces, (4) the resonant frequencies of concrete specimens, (5) the dynamic modulus of elasticity from the fundamental flexural, longitudinal and torsional frequencies of cylindrical and prismatic specimens. Nevertheless, it is not possible to find a standard that regulates the tests on asphalt concrete cylindrical samples/specimens to derive, at the same time, the mechanical impedance and the acoustic response. For this reason, a new testing procedure was set up in this study through preliminary tests (see section 2.2), and subsequently applied during the main tests (see section 3).

It is important to underline that several mechanistic properties (e.g., moduli, ratio of stress to strain) are intrinsic properties of materials, while others (e.g., stiffness, ratio of force or stress to displacement) depends on geometry and this implies the need for specifying sample geometry (cf. EN 29052-1 [40]) as well as the remaining boundary conditions (such as additional load plates, plastic foils, paste of plaster of Paris, excitation and measuring devices).

Different FRFs of a loaded system can be derived from imposed loads (e.g., forces or displacements), and produced mechanical responses (i.e., acceleration, or velocity and displacement derived from the acceleration) [39], [45]. Note that it is possible to attach an accelerometer at a particular point of a structure and excite the structure at another point with a force gauge instrumented hammer. By measuring the excitation force and the response, the resulting frequency response function describes the relationship between those two points of the structure as a function of frequency [46]. The concept of transfer function, H, helps understand the concept of FRF. A basic equation for H is:

$$H(f) = \frac{Y(f)}{X(f)} \tag{1}$$

where $H(f)$ is the transfer function, $Y(f)$ is the output of the system in the frequency domain, and $X(f)$ is the input to the system in the frequency domain [46]. As mentioned above, an example of FRF is the Mechanical Impedance (MI), which represents the ratio between the sinusoidal force applied to the system and the velocity produced by the aforementioned force [47].

Importantly, vibrating systems are affected by the damping coefficient (c). This latter is usually expressed in Ns/m and governs the response of systems at natural frequencies. Higher damping coefficients correspond to lower deflections.

Other damping-related parameters are the damping ratio, the loss factor, the percent of critical damping, and the phase angle between cycling stress and strain:

$$\eta = \frac{f_2 - f_1}{2f_0} = \zeta = \frac{damping}{critical\ damping} = \frac{1}{2Q} = \frac{\%Cr}{50} = tan\phi = \frac{\Delta\omega_{3dB}}{\omega_0} \quad (2)$$

Note. %Cr represents the percent of critical damping and not the percent of Crumb Rubber (%CR)

where η is the loss factor (dimensionless); ζ is the damping ratio, (dimensionless; which is given by the actual damping, i.e. the damping coefficient, divided by the critical damping, i.e. equal to $2\cdot(km)^{0.5}$ in the simplest case [48]); Q is damping factor or quality factor (dimensionless). Finally, $\%Cr$ is the percent of critical damping ($\%Cr = 100\cdot\zeta$), while ϕ is phase angle between cyclic stress and strain, $\Delta\omega_{3dB}$ is the frequency range of 3 dB decay in radians and ω_0 is the resonance frequency in radians.

Note that the reciprocal of the damping factor (or quality factor) equals twice the damping ratio and both this and the damping factor are dimensionless. Furthermore, being c and ζ proportional, this implies that high damping corresponds to low *Q*s. For damping estimates, note that in a FRF, the damping is proportional to the width (f_2 - f_1) of the resonant peak about the peak's centre frequency, f_0 ("3 dB method", also called "half power method" [49,50]; see Figure 2):

$$Q = \frac{f_0}{f_2 - f_1} \quad (3)$$

where f_0 is frequency of resonant peak (Hz), f_2 is the frequency value (Hz) 3 dB down from peak value (higher than f_0), and f_1 is the frequency value (Hz) 3 dB down from peak value (lower than f_0).

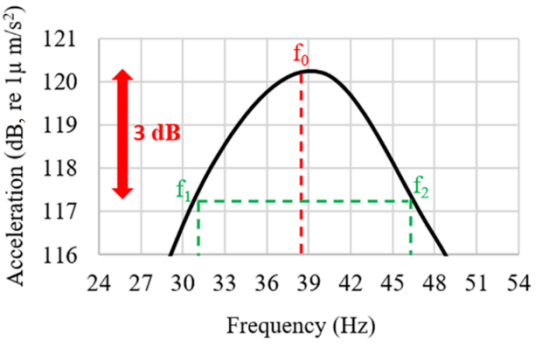

Fig. 2. Evaluation of quality factor Q

Table 1 illustrates the main result of Task 1, i.e. basic information on several FRFs of interest related to different types of road pavement materials. Note that damping factors of metal structures such as airplane fuselages are lower than 0.05, while automotive suspensions are often in the range of 0.2-0.3. According to Uglova and Tiraturyan [51], pavement layers damping ratios range from 0.03 to 0.23, while Hasheminejad et al. [52] found values ranging from 0.01 to 0.34.

Table 1

Mechanical impedance, dynamic stiffness, and stiffness modulus for different types of pavement materials

Parameter	What it is	Example of values	Reference
Apparent Dynamic Stiffness *per* unit area of the tested specimen, *s't*, (RM, EN 29052-1, MPa/m)	Ratio of dynamic force on dynamic displacement per unit area. It can be estimated through the corresponding resonant frequency *fr:* $s'_t = 4\pi^2 m'_t f^2 r$	185-359 MPa/m (HMA) 1436-3484 MPa/m (SMA)	[53] [54]

Dynamic Stiffness spectrum (NRM)	Ratio of dynamic force on dynamic displacement. It represents a frequency spectrum.	17234 kN/m (SMA, maximum value of the spectrum)	[54]
Mechanical impedance, MI	Ratio of dynamic force on dynamic speed. It represents a frequency spectrum.	1-200 kNs/m (HMA)	[54] [55]
Mechanical impedance, MI	Ratio of dynamic force on dynamic speed. It represents a frequency spectrum.	0.1-3.2 kNs/m (PERS)	[34]
Max MI	Max value in the corresponding MI spectrum in 50-1250Hz.	50-350 kNs/m (HMA)	[55]
Damping ratio, ζ	Actual damping (damping coefficient) divided by critical damping, $2\cdot(km)^{0.5}$	0.01-0.34	[52] [51]

Note. HMA: Hot Mix Asphalt; RM: Resonant Method; NRM: Non-Resonant Method; SMA: Stone Mastic Asphalt; PERS: PoroElastic Road Surface; MI: Mechanical Impedance.

5. Preliminary tests to set up the system and a new testing procedure

5.1 System set up

The first scope of the preliminary tests carried out in this study was to set up the testing system. Accordingly, in this phase of the study (Tasks 2.1 and 2.2), measurements were carried out on cylindrical samples and on rectangular slabs using an ad hoc equipment that is able to produce a known force, to gather the seismic response (acceleration) and the road acoustic response (RAR, air-borne sound pressure) generated by each hammer hit. The equipment includes (see Figure 3):

a) Impact hammer 'Bruel & Kjaer Type 8206' to register the applied force;
b) Piezoelectric accelerometer 'Bruel & Kjaer Type 4507' with a frequency range of 0.3-6000 Hz;
c) Omnidirectional pre-polarized microphone 'Audix TM1'with a frequency response of 20 Hz-25 kHz +/- 2 dB, sensitivity of 6 mV/Pa @1 kHz, maximum SPL of 130 dB with distortion <1 % 140 dB max and dynamic range of 112 dB;
d) External sound card 'Roland quad-capture UA-55';
e) Laptop computer;
f) Bruel & Kjaer front-end acquisition board, used to convert the hammer's time series to frequency responses (using the Fast Fourier Transform, FFT).

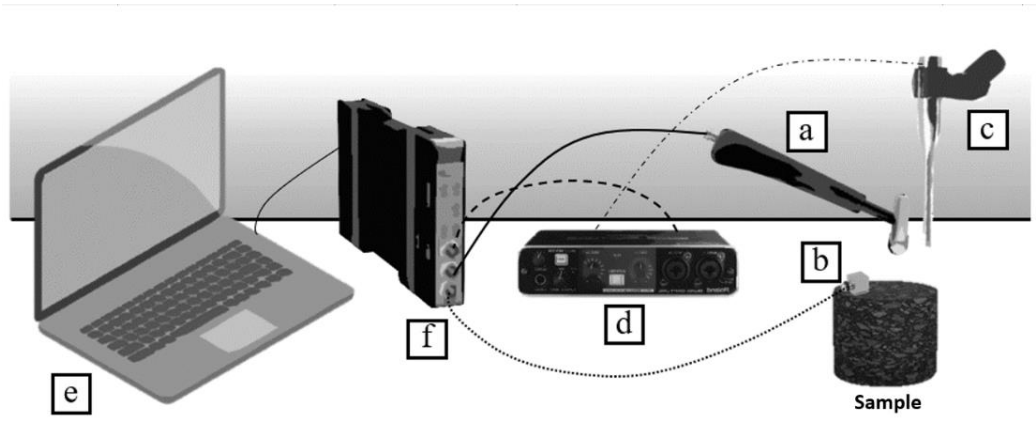

Fig. 3. Measurement chain (refer to the text for explanation of the parts 'a' to 'f')

Each impact hammer test included several hits. The middle of the upper surface of samples was hit. Hits were applied on a load plate or directly on the upper face of the specimens and the mechanical impedance (based on force and velocity) and the dynamic stiffness (based on force and displacement) were derived.

Results were analysed in terms of a multiple degree of freedom system (MDoF) to assess inference reasonableness. To this end, it is noted that while each sample is basically a mass-spring-damper system with a Single Degree of Freedom (SDoF), actual tests were carried out with samples located on a pavement, with or without load plate and gypsum plaster (MDoF system).

Subsequently, the dynamic stiffness (spectrum and resonant values) was compared with the one derived based on a vibration system model of springs in series, where the equivalent stiffness is given by k_{eq}. Each "stiffness" of the spring series was estimated as a function of the Young's modulus, the thickness, and its radius. In turn, moduli were assessed based on the literature and based on in-lab expedite measurements.

In the end, it was possible to set up the new testing procedure (method) and to compare it with the one reported in the standard EN 29052-1 (in case of cylindrical samples) and in the standard ISO 7626-5 (in case of slabs). The proposed method complies with the one set up in the standards mentioned above, and can be also applied for testing samples consisting of different materials and having different geometries.

5.2. New testing procedure set up

The second scope of the preliminary tests carried out in this study was to set up a new testing procedure suitable to derive both the mechanical impedance (MI) and the road acoustic response (RAR) of cylindrical samples/specimens. Consequently, several tests were carried out involving three types of materials (Hot Mix Asphalt, HMA, Crumb Rubber and resin, CR&Resin, and steel), and applying two standardized testing procedures, i.e. one for cylindrical samples (EN29052-1), and one for slabs (ISO 7626-5), using different boundary conditions. At the end of the tests, 26 different measurement configurations were used.

Table 2 reports the characteristics of the samples used for each material (average dimensions are shown). The testing procedures, details about the configurations mentioned above and the results related to the preliminary tests to set up the new testing procedure are described and presented in the following.

Table 2

Samples used during the preliminary tests

ID sample	Material	Geometry	Length (mm)	Width (mm)	Radius (mm)	Thickness (mm)
P01-B	HMA	Slab	520	360	-	50
P02	CR&Resin	Slab	500	350	-	50
P04	Steel	Slab	500	260	-	16
C02	CR&Resin	Cylinder	-	-	53	49
C03	HMA	Cylinder	-	-	47	51
C04	HMA	Cylinder	-	-	47	43

As mentioned above, the preliminary tests were carried out on 26 cases, involving different types of materials and different boundary conditions that can be summarized as follows:

- Shape and dimensions of the sample system (cylindrical, squared, horizontal dimensions in the range 0.2 m ± 0.1 m).
- Layers involved:
  - presence or absence of gypsum layers (cf. [53] and EN 29052-1 [40]);
  - presence or absence of a steel plate on the top (load plate), between hammer and sample. Indeed, for applying the Resonant Method, it is suggested to place a mass on the top of the studied surface [54]. Importantly, the cases with an upper mass were not considered in terms of acoustic response of the sample under test.

- Hammer heights: the samples were hit using the hammer, whose tip was dropped from a height that varies between 100 mm and 180 mm.

Testing procedure EN29052-1: for cylindrical samples, a testing procedure based on the standard EN29052-1 was used. This procedure consists of the following steps:

1. Laying down a layer of gypsum on the ground/pavement (to level the sample);
2. Placing a plastic film on the gypsum (to avoid that sample and gypsum touch each other) and attaching it on the ground using scotch tape;
3. Placing the sample on the plastic film (before the plaster hardens), pressing and levelling the sample toward the gypsum, and letting the gypsum drying;
4. Repeating steps 2 and 1 on the top face of the sample (note that this step was bypassed in some configurations, such as those aimed at gathering the acoustic response of the sample to a given load);
5. Placing a cylindrical metallic plate on the top of the sample (note that tests with and without the load plate were carried out to understand its influence of this factor on the mechanical response of the sample);
6. Attaching a mono-axial accelerometer on the top of the sample (or, when used, on the load plate), and connecting the accelerometer to the other devices shown in Fig. 3;
7. Placing a microphone close to the top of the sample and connecting it as shown in Fig. 3 (when the load plate was not used);
8. Hitting the sample using the impact hammer from different heights;
9. Recording the output signals from hammer (force), accelerometer (acceleration) and microphone (acoustic response) when used;
10. Processing the recorded signals in order to derive the predefined FRFs.

Testing procedure ISO 7626-5: for slab samples, a testing procedure based on the standard ISO 7626-5 was used. This procedure consists of the following steps:

1. Placing the slab sample on the ground;
2. Attaching a mono-axial accelerometer on the top of the sample slab, and connecting the accelerometer to the other devices shown in Fig. 3;
3. Placing a microphone close to the top of the sample diametrically opposite to the accelerometer and connecting it as in Fig. 3;
4. Hitting the sample using the impact hammer, in such a way that the hammer falls down from a given height and the face of the hammer's tip is parallel to the sample's face;
5. Recording the output signals from hammer (force), accelerometer (acceleration) and microphone (acoustic response);
6. Processing the recorded signals in order to derive the predefined FRFs.

Based on tests, the results in Fig. 4 were obtained. Note that different spectra are illustrated, due to the boundary conditions adopted, i.e. the presence or not of a load plate, the presence or not of a thin layer of gypsum between the sample and the pavement, sample geometry, and the type of underlayer.

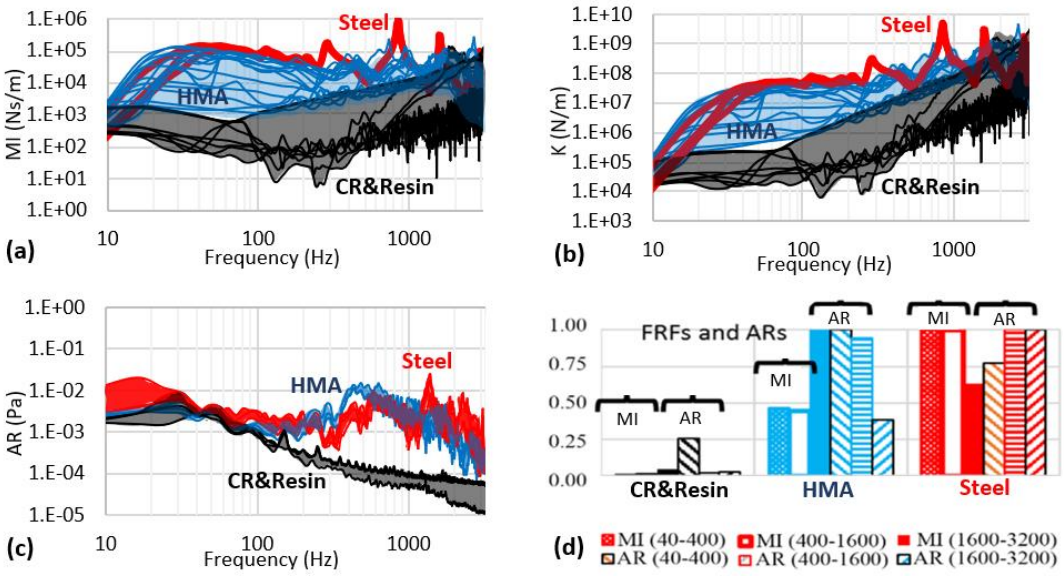

Fig. 4. (a) MI, (b) K, (c) AR spectra and (d) average values for different materials

Based on Fig. 4, the following points can be highlighted:

1) by referring to natural frequencies (dips in the spectra of dynamic stiffness, *K*, and of mechanical impedance, *MI*), note that each frequency can be used to derive a corresponding stiffness, being the natural (angular) frequency of a mass-spring-damper system the square root of the stiffness divided by the mass (resonant method [54]). Furthermore, note that the stiffness of each part of the vibrating system (including the sample under analysis) contributes to the k_{eq} above;
2) the presence of a steel load plate on the top of the specimen does not affect significantly *MI* and *K* (variations lower than 5 % in terms of *MI* and frequency can be detected);
3) even if the depth is the same, the remaining dimensions (slab or cylindrical sample) affect *MI* and *K*. Higher surfaces (starting from a small sample) imply lower deflections and on average higher MIs;
4) the first natural frequency (dip) of CR & resin samples ranges from 30 Hz to 130 Hz. The first natural frequency of HMA samples ranges from about 130 Hz to about 260 Hz. A natural frequency of steel samples around 400-600 Hz is usually detected;
5) in terms of differences and features mostly related to materials, note that i) HMAs have often FRF values (*MI*, *K*) that are intermediate between the ones of CR & resin and Steel. ii) HMA peaks (lower speeds) are often about 400 Hz higher than the ones of MI and K. iii) CR content decreases the medium- and high-frequency values of *MI*, *K*, and road acoustic response (*RAR*, with respect to HMAs). iv) For a given material, the distance between lower and upper envelope (along the y-axis) varies as a function of frequency (x-axis) and material. To this end, it is noted that lower differences (lower-to-higher envelope) are associated to steel, while higher ranges are associated to HMAs. v) Overall, the lower the frequency is, the lower the response variability (i.e., of *MI*, *K* and *AR*) is.
6) Figure 4d refers to the average values of FRF and AR obtained for the given material (e.g., HMA) and for the given frequency range (e.g., 40-400Hz). Values are normalised in 0-100%. Note that CR&Resin samples have the lowest values of AR and MI, while Steel samples have the highest ones. Importantly, while HMA AR in 1600-3200Hz is HMA lowest AR, for steel samples, the lowest AR is the one that refers to low frequencies. Indeed, HMA AR decreases for high frequencies (1600-3200Hz) while steel AR decreases for low frequencies (40-400Hz). Finally, the acoustic response, *AR*, of the CR-based material is lower than the *AR* of the remaining materials (HMA and steel).

New testing procedure. Based on the preliminary tests and the results listed above and shown in Fig. 4, the following new testing procedure was defined and used to test the CR-added mixtures (see Task 3):

1) Laying down a layer of gypsum with thickness of about 2 mm on the ground (to level the sample);

2) Placing a plastic film on the gypsum (to avoid that sample and gypsum touch each other) and attaching it on the ground using scotch tape;
3) Placing the sample on the plastic film (before the plaster hardens), pressing and levelling the sample toward the gypsum, and let the gypsum drying;
4) Attaching a mono-axial accelerometer on the top of the sample, 20 mm far from the point of the impact (centre of the sample surface), and connecting the accelerometer to the other devices as shown in Fig. 3;
5) Placing a microphone close to the top of the sample diametrically opposite to the accelerometer, at a height of 50 mm, far from the hitting point, and connecting it as in Fig. 3;
6) Hitting the sample using the impact hammer, equipped with a plastic tip (medium hardness), in such a way that the hammer falls down from a given height and the face of the hammer's tip is parallel to the sample's face;
7) Recording the output signals from hammer (force), accelerometer (acceleration) and microphone (acoustic response), and, in order to reduce the measurement error, repeating the number of measurements until an acceptable spread (low variance) in the results is obtained. For each sample, measurements end when the set of signals recorded has a "stable average", i.e. there is a set of signals that is characterized by spectra that have similar variance, considering the variance of the i-th spectrum with respect to the average spectrum);
8) Processing the recorded signals in order to derive the predefined FRFs (e.g., mechanical impedance).

6. Mixture design and sample production

In Task 3, the design of the asphalt concrete mixtures and the production of the related samples used were carried out. The choice of the HMA composition was based on the literature [22,56,57]. In this task attention was focused on the relationship between energy (based on hammer drop height, *Hh*), crumb rubber percentage (%*CR*), road acoustic response, *RAR*, and FRFs (cf. section 1.3). Four types of mixtures were produced and tested in the laboratory (cf. Tables 3-8 and Figs 5-9).

Asphalt binder percentage was designed based on mineral aggregate and crumb rubber specific surface under the following hypotheses (cf. [58,59]):

- The total quantity of asphalt binder includes two main parts: the one that covers CR particles and the one that covers mineral aggregate.
- As is well known, the richness modulus depends on the surface area (of particles) per unit weight of the material (i.e., the specific surface) and is the factor that links asphalt binder percentage to the specific surface raised to the power of 0.2. In this case (use of CR, dry method), the richness modulus equation must be corrected to consider the different specific gravities of particles (rubber versus mineral aggregates).

The following equation was derived and used:

$$\frac{Pb}{\sum Pa_i} = \sum_1^N \lambda_i \cdot \frac{{SS_i}^{0.2}}{G_{sb}} \quad (4)$$

Equation (4) refers to the relationship between the percentage of bitumen ($P_b/\Sigma Pa_i$, w/w, referred to aggregates) and the specific surface of aggregates, SS_i, where the subscript i refers to the i-th class/type of aggregates (cf. [58,59]). G_{sb} refers to the specific gravity of aggregates and λ_i is a coefficient to calibrate that includes the richness modulus defined in [77]. Note that herein the term aggregates stand for mineral aggregates and other particles (such as CR).

Figure 5 summarises samples gradation and production, with the gyratory compactor 'Rainhart' (EN 12697-31:2019) (left) and how sample characteristics (i.e., %*CR*, *AV* and Geometry) and impulsive force (*F(f)*) affect impact energy (*E**), road acoustic response (*RAR*), time response functions (TRF), and FRFs (right).

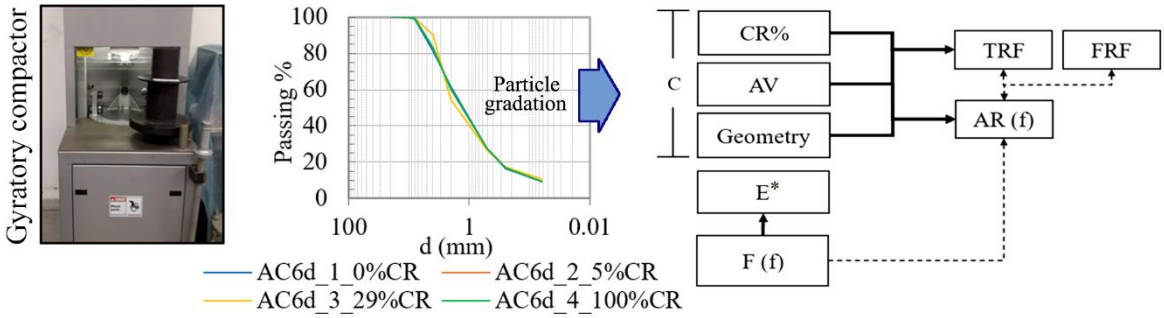

Note. Particle gradation: gradation of mineral aggregates and CR. CR%: crumb rubber percentage; AV: air voids; E*: energy; F: force; MI: mechanical impedance; AR: acoustic response; f: frequency; TRF: time response function; FRF: frequency response function.

Fig. 5. RAR and MI dependence on mixture and impact energy

Based on the considerations above and considering the results of the study of Kragh et al. [26]), different mixes were designed by varying the percentage of CR included (particle size of 2-4 mm) and using the dry method (cf. Table 3 and Figs 5 and 6). The first mixture (AC6d_1) is a AC6d as in [26] (i.e., without CR), while the other mixtures (AC6d_2, AC6d_3, and AC6d_4) were designed replacing a given percentage of aggregates (5 %, 29 %, and 100 %, respectively) with CR. Hence, the produced samples were called using the term "AC6d". Note that three samples for each mixture were produced (averages characteristics are reported in Table 3). The type of bitumen used is a 'Eni paving grade bitumen 50/70' with: a) penetration at 25°C = min 50/max 70 [1/10 mm] (EN 1426:2015); b) softening point, ring & ball = min 46/max 54 [°C] (EN 1427:2015); c) dynamic viscosity at 60°C = 145 [Pas] (EN 12596). Air voids have been determined according to EN 12697-5:2019, EN 12697-6:2012, EN 12697-8:2018. Furthermore, three samples composed by styrene-butadiene rubber (SBR) and ethylene propylene rubber (EPDM), compacted using a polyurethane glue in a hot process, were used as reference samples (herein called "100%CR resin"). Note that in this case the samples were not produced by the authors of this study.

Table 3

Characteristics of the fifteen samples produced in the laboratory and of the "100%CR resin" (averages of three values per mixture).

Mix ID	AV (%)	CR/(CR+A) (w/w) (%)	CR/A (w/w) (%)	CR/A (V/V) (%)	Sample dimensions (thickness · diameter) [mm · mm]	Sample mass [kg]	Number of samples produced and/or tested
AC6d_1 (reference)	4	0	0	0	115 · 97.5	2.052	3
AC6d_2	18	5	5.3	13	133 · 97.5	1.906	3
AC6d_3	24	29	42	100	186 · 97.5	1.905	3
AC6d_4	31	100	-	-	172 · 97.5	0.987	3
100%CR resin (reference)	48	100	-	-	155 · 100	0.606	3

Symbols. CR: crumb rubber; A: mineral aggregates; B: bitumen; AV: air voids. *Note:* Based on the standard EN 12697-5:2019, the following percentages of bitumen (w/w, referred to weight of CR+A) were used for the four mixtures AC6d_1 to AC6d_4, respectively: 6.3, 6.6, 7.5, and 8.7.

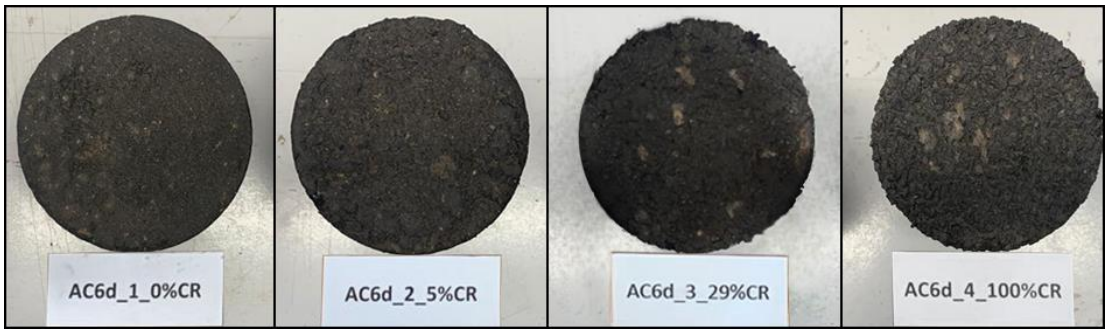

Fig. 6. Four out of fifteen samples produced in the laboratory ("AC6d_1_0%CR" does not contain CR, while the others contain 5 %, 29 %, and 100 % of CR)

Note that, before the main tests carried out in this study, the samples were cut in order to have the same height (115 mm).

7. Results and discussions

This section of the paper reports the results of the main tests of the study. Figures 7-9 and Tables 4-6 illustrate the results obtained in Task 3.

It is important to highlight that the plots reported below refer to measurements which were:

- Carried out applying the new testing procedure (defined at the end of section 5), on fifteen specially produced cylindrical samples (consisting in twelve samples with CR and three without CR; see Table 3), and, for further comparisons, on three samples consisting of CR (100 % of the aggregates and resin as a binder, herein called "100%CR resin");
- Repeated twice (i.e., by two different operators) until more than 10 set of signals (forces, accelerations, acoustic responses) were recorded per sample and per operator;
- Carried out using proper measurement settings, which allowed gathering the signals of the samples under test and deriving the related spectra with a sufficient resolution. In particular, the following main settings were used: sampling rate = 8192 samples *per* second, frequency resolution = 8 Hz, time weighting = Hanning, overlap between consecutive time records = 66.7%.

Each operator did the following steps for each sample:

1. Recorded three sets of signals (i.e., twenty-five forces, twenty-five accelerations, and twenty-five acoustic responses);
2. Calculated the spectra (using the Fast Fourier Transform, FFT) related to the signals from step 1;
3. Calculated three average spectra from the spectra from step 2 (i.e., one for forces, one for accelerations, and one for acoustic responses);
4. Calculated the variance of each spectrum from step 2 with respect to the average spectra at point 3;
5. Found the ten spectra (out of the twenty-five above) with the lowest values of variance for each type of signal (ten for forces, ten for accelerations, and ten for acoustic responses);
6. Calculated the average spectrum from the ten spectra from step 5 for the given type of signal (i.e., one spectrum for forces, one for accelerations, and one for acoustic responses);
7. Derived the three average signals (time domain) from the spectra from step 6 (i.e., one for forces, one for accelerations, and one for acoustic responses).

Finally, considering both the operators, the average signal *per* type (e.g., from two acceleration signals to one in the time domain) and the average spectrum *per* type (e.g., from two acceleration signals to one in the frequency domain) were calculated *per* sample and *per* type of signal.

Fig. 7 shows the average signals for deflection (derived from the average acceleration), velocity (derived from the average acceleration), acceleration, and the average spectra of the mechanical impedance (derived from the force and acceleration) of the samples under test.

Based on Fig. 7, samples with high percentages of rubber show particular features in in terms of time- and frequency-related plots. Particularly, higher speeds imply lower *MIs*, especially for low frequencies.

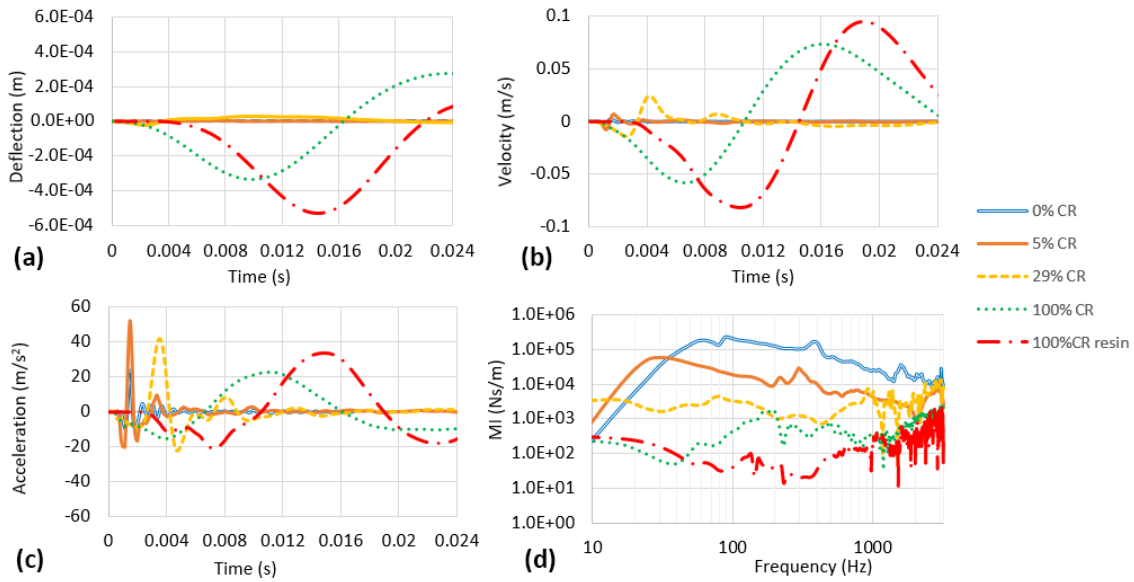

Fig. 7. (a) Acceleration, (b) velocity, (c) deflection, (d) mechanical impedance

Fig. 8a illustrates 1) *MI* values for CR percentages of 0%, 5%, 29%, and 100% (with respect to the mass of aggregates and CR). 2) The lines representing the stiffness-to-frequency ratio *K/f* (low frequencies, response below the natural frequency f) for each class of mixes. 3) The lines representing the product mass by frequency *m*f* (high frequencies, response above the natural frequency, *f*). The estimate of damping (response at the resonant frequency), is reported in Table 4. For this latter, note that higher *%CR* yield a higher damping and a lower quality factor (*Q*).

For Fig.8b, equation 5 shows how *RAR* varies as a function of *%CR* and Energy (in terms of drop height, *Hh*). A suitable compromise between precision and simplicity is obtained through the following equation:

$$max\ RAR\ =\ [A \cdot (100 - \%CR)^B + C] \cdot [exp\left(\frac{Hh}{D}\right) - 1] \quad (5)$$

where *max RAR* (Pa) is the maximum value of *RAR*, *Hh* (cm) refers to the drop height (and then to the energy of the impact), *%CR* is the percentage of CR (between 0 and 100), and *A*, *B*, *C*, *D* are coefficients to calibrate (e.g., *A* = 3E-03, *B* = 5.4, *C* = 2E10, and *D* = 3E9).

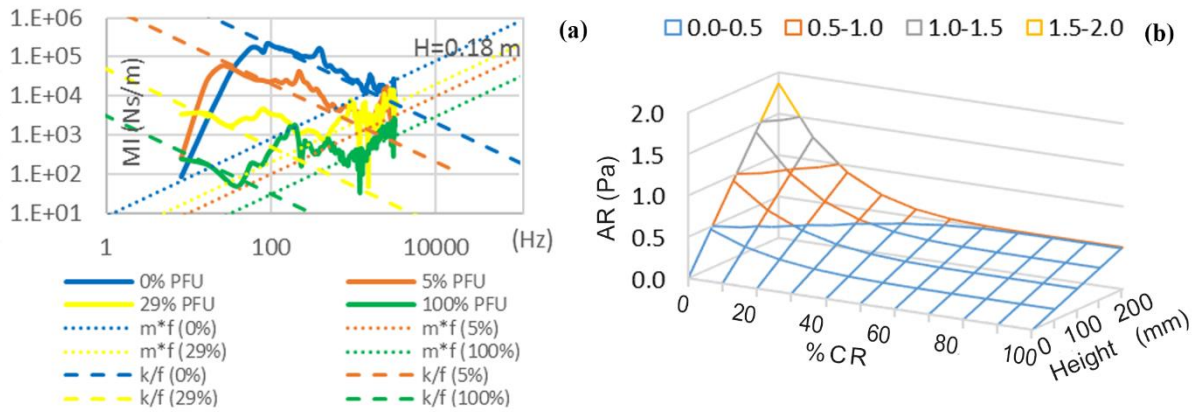

Fig. 8. (a) Mechanical Impedance, m*f and k/f; (b) max RAR as a function of hammer drop height and CR percentage

The results of the damping ratio, ζ, in percentage, presented in Table 4 refer to the case of higher energy (180 mm hammer height). Note that for CR = 0% and CR = 5%, the proximity of two closely spaced modes made the determination of *Q* via the "3 dB method" more difficult. Note that the damping ratio was calculated [49,50] using the "3 dB method", also called "half power method". Finally note that deflections range from 0.3-0.5 mm (only CR) to 0.0007 mm (HMA), while the deflections under a traditional car (HMA pavement) may be about 0.03 mm.

Table 4

Impact of %CR (@180 mm hammer drop height case)

CR/(CR+A) (w/w)	Binder	max F	max d	max v	max a	max RAR	ζ	max F /max v	max F /max d	Resonance
(%)		(N)	(m)	(m/s)	(m/s^2)	(Pa)	(%)	(Ns/m)	(N/m)	(Hz)
0	B	130	6.67E-07	0.002	23.68	1.2	10	5.9E+04	2.0E+08	205
5	B	87	3.23E-06	0.008	52.20	0.24	10	1.1E+04	2.7E+07	192
29	B	57	2.07E-05	0.024	41.89	0.19	14	2.3E+03	2.8E+06	216
100	B	17	3.35E-04	0.073	22.65	0.09	20	2.3E+02	5.1E+04	40
100 (with resin)	Re	16	5.28E-04	0.082	39.02	0.09	20	2.0E+02	3.1E+04	53

Note. CR: crumb rubber; F: force; d: deflection; v: velocity; a: acceleration; RAR: road acoustic response; ζ: damping ratio; B: asphalt binder.

Table 5 refers to Pearson coefficients and illustrates that 1) The higher the CR percentage is, the higher the deflection is. 2) The higher the speed is, the lower the acceleration is. 3) Vice versa, lower values of CR percentages imply higher noise and lower damping ratios. Table 6 still illustrates the Pearson coefficients and refers to the values of *MI* and *K*, for the samples considered in Table 5, except that for the case of 100 % CR with resin.

Table 6 shows that the RAR@400-1600 Hz (that is very relevant to human receptors) are well correlated to *MI* and *K* for frequencies in 400-3200 Hz, and to accelerations *(a)*, speeds *(v)*, and deflections *(d)* for 1600-3200 Hz. These results appear to highlight the importance of FRFs, whereas quasi-static interactions (e.g., *MI* when f→0) appears less important in terms of acoustic response.

Table 5

Pearson coefficients

	%CR	max F	max d	max v	max a	max RAR	ζ	max F/max v	max F/max d
%CR	1.0	-0.9	1.0	1.0	-0.5	-0.6	1.0	-0.6	-0.6
max F		1.0	-0.8	-0.9	0.1	**0.9**	-0.9	0.9	0.9
max d			1.0	1.0	-0.6	-0.5	0.9	-0.5	-0.4
max v				1.0	-0.5	-0.6	1.0	-0.6	-0.6
max a					1.0	-0.4	-0.5	-0.4	-0.4
max RAR						1.0	-0.5	**1.0**	**1.0**
ζ							1.0	-0.6	-0.5
max F/max v								1.0	1.0
max F/max d									1.0

Note. %CR: crumb rubber by total weight; F: force; d: deflection; v: velocity; a: acceleration; RAR: road acoustic response; ζ: damping ratio.

Table 6

Pearson coefficients between *RAR* and *MI*, *K*, *a*, *v*, and *d* (@180 mm hammer height case)

RAR@	**MI1**	**MI2**	**MI3**	**MI4**	**K1**	**K2**	**K3**	**K4**				
0-40 Hz	0.39	0.98	0.98	0.93	0.56	0.99	0.98	0.89				
40-400 Hz	0.43	0.98	0.99	0.96	0.62	1.00	0.99	0.93				
400-1600 Hz	0.60	1.00	1.00	0.97	0.56	0.98	0.99	0.98				
1600-3200 Hz	0.51	1.00	1.00	0.97	0.60	1.00	1.00	0.96				
	a1	**a2**	**a3**	**a4**	**v1**	**v2**	**v3**	**v4**	**d1**	**d2**	**d3**	**d4**
0-40 Hz	-0.26	-0.29	-0.09	0.45	-0.27	-0.40	-0.41	0.55	-0.27	-0.31	-0.54	0.51
40-400 Hz	-0.36	-0.38	-0.06	0.48	-0.36	-0.48	-0.34	0.58	-0.36	-0.40	-0.46	0.54
400-1600 Hz	-0.47	-0.47	0.13	0.64	-0.48	-0.62	-0.17	0.72	-0.48	-0.52	-0.33	0.70
1600-3200 Hz	-0.41	-0.43	0.03	0.56	-0.42	-0.55	-0.26	0.65	-1.00	-0.99	-0.33	1.00

Note. MI: mechanical impedance; MI1: @0-40 Hz; MI2: @40-400 Hz; MI3: @400-1600 Hz; MI4: @1600-3200 Hz; K: dynamic stiffness; a: acceleration; v: velocity; d: deflection; The numbers 1, 2, 3, and 4 refer to the four samples mixture used in this study.

Many factors suggest to be cautious in drawing conclusions from the above in terms of tyre/road noise, including what follows:

- Differences in terms of power transmitted to the pavement/sample (e.g., hammer drop height *versus* tyre and vehicle type and conditions).
- Scale effects (e.g., due to the different dimensions of the couples: sample *vs.* pavement, hammer tip *vs.* tyre rubber tread element).

- Type of contact and surface (e.g., due to differences related to materials and shapes of the couples: hammer tip *vs.* tyre).

Under the conditions and the limitations of the study mentioned above, the SPL recorded here as max AR (90-101 dB, which was measured using a microphone placed at 50 mm) could be compared to the SPL measured through the CPX method with the vehicle driven at 80 km/h (about 95-100 dB, using microphones at 200-300 mm from the source).

8. Conclusions

Based on results and data interpretation, the following conclusions can be drawn:

1) The aim of this study and the related laboratory tests was to study the correlation between the Frequency Response Functions (FRFs) and the Acoustic Response of the Road (herein called *RAR*) of flexible road pavements (where surface courses are bituminous mixtures). In more detail, the possibility of having sound radiation from the road, which may be of significance in tyre/road noise emission, was investigated. Therefore, the *RAR* of asphalt concrete specimens was studied together with their FRFs.
2) Many parameters affect the FRF estimates (e.g., sample geometry, air voids, and under-layer materials).
3) In the literature, different standards are reported in order to obtain FRFs (e.g., dynamic stiffness, *K*, and mechanical impedance, *MI*). Nevertheless, there are no standards that refer to the tests on asphalt concrete cylindrical samples/specimens and this is a weak point.
4) The EN 29052-1 seems to provide quite sound estimates of resonant frequencies for cylindrical samples, especially in case of CR-added mixtures, where their weakest mechanistic properties positively impact estimates. MDoF systems are useful to control experimental results.
5) For the mixes investigated and for the highest impact energy under investigation, an increase of CR percentage and the corresponding variations in terms of air voids imply the decrease of *MI*, of stiffness, and of max RAR.
6) In more detail, the synergistic influence of the hammer drop height (*Hh*) and the corresponding equations (*RAR* as a function of %CR and Hh) have been studied. Other experiments are needed to support these results.
7) Based on measurements, *MI* and *K* appear to be sound indicators to evaluate the *RAR* for frequencies in the range 400-3200 Hz. It should be underlined that the *RAR* could be influenced by the air void content of the samples.
8) The CR-related "mechanistic" contribution to low *RARs* appears to be scientifically supported. For low percentages of CR, the assessment of CR actual impact on *RAR* calls for further research.
9) Based on results, the mixtures with high percentages of CR outrank the remaining ones in terms of minimisation of the *RAR*. It is noted that many issues still call for further investigation, such as CR gradation, optimal binder percentage and type, technology used, and environmental balance. These factors, together with the increase of cost with quite high CR percentages, add complexity to the selection of the best solution.
10) By referring to RAR-based *versus* CPX-based inferences and analogies, the relationship between the *RAR*, herein defined and measured, and the on-site CPX emerges as mainly unknown and probably quite complex. Nevertheless, other research reported in the literature has indicated that pavement stiffness has a substantial influence also on CPX noise levels, provided that CR percentages are quite high. Importantly, at least for small or moderate impact energies, the actual effect of low percentages of CR on common asphalt rubber pavements when impacted by tyre treads calls for further research and investigation.
11) Further investigations are required to have a higher accuracy of the results and to better understand CR actual impact on tyre/road noise and remaining properties. The RAR studied here could have an effect on tire / road emissions from vehicles or test tires, but, unfortunately, this effect cannot be fully determined from the results presented in this study. Thence, either a further theoretical model or a complex set of experiments is required for having a single-factor approach and controlling different known or suspected sources of variation (including texture and air voids).

References

[1] R. Calejo Rodrigues, Traffic noise and energy, Energy Reports. 6 (2020) 177–183. doi:10.1016/j.egyr.2019.08.039.

[2] WHO Europe, Burden of disease from environmental noise: quantification of healthy life years lost in Europe, Copenhagen, Denmark, 2011.

[3] F.G. Praticò, Roads and Loudness : a More Comprehensive Approach, Road Mater. Pavement Des. (2011) 359–377. doi:10.1080/14680629.2001.9689908.

[4] T. Li, Influencing Parameters on Tire–Pavement Interaction Noise: Review, Experiments and Design Considerations, Designs. 2 (2018) 38. doi:10.3390/designs2040038.

[5] F.G. Praticò, On the dependence of acoustic performance on pavement characteristics, 29 (2014) 79–87. doi:10.1016/j.trd.2014.04.004.

[6] R. Fedele, F.G. Praticò, R. Carotenuto, F.G. Della Corte, Energy savings in transportation: setting up an innovative SHM method, Math. Model. Eng. Probl. 5 (2018) 323–330. doi:10.18280/mmep.050408.

[7] F.G. Praticò, R. Ammendola, A. Moro, Factors affecting the environmental impact of pavement wear, Transp. Res. Part D Transp. Environ. 15 (2010) 127–133. doi:10.1016/j.trd.2009.12.002.

[8] D. Covaciu, D. Florea, J. Timar, Estimation of the noise level produced by road traffic in roundabouts, Appl. Acoust. (2015). doi:10.1016/j.apacoust.2015.04.017.

[9] U. Sandberg, Ś.Ż. Beata, J.A. Ejsmont, Tyre / road noise reduction of poroelastic road surface tested in a laboratory, (2013) 1–8.

[10] W. Keulen, M. Duskov, Inventory Study of Basic Knowledge on Tire/Road Noise (Report number: DWW-2005-022), 2005.

[11] SIEMENS, What is a Frequency Response Function (FRF)?, Siemens Simcenter. (2019) 1–12.

[12] The SMILE Commission, Guidelines for road traffic noise abatement, 2003.

[13] European Commision, FUTURE BRIEF: Noise abatement approaches Science for Environment Policyscience-environment-policy 1. Noise pollution: a growing environmental concern 1.1 Human health effects 1.2 Policy context 2. Noise mitigation 2.1 Traffic noise 2.2 Railway noise 2.3 A, 2017. doi:10.2779/016648.

[14] U. Sandberg, J.A. Ejsmont, Tyre/Road Noise Reference Book, 2002. https://www.informex.info/html/book__tyre_road_noise_.html.

[15] S. Mavridou, F. Kehagia, Environmental Noise Performance of Rubberized Asphalt Mixtures: Lamia's case study, Procedia Environ. Sci. 38 (2017) 804–811. doi:10.1016/j.proenv.2017.03.165.

[16] A. Vaitkus, D. Čygas, V. Vorobjovas, T. Andriejauskas, Traffic/Road Noise Mitigation under Modified Asphalt Pavements, in: Transp. Res. Procedia, 2016: pp. 2698–2703. doi:10.1016/j.trpro.2016.05.446.

[17] A. Vaitkus, V. Vorobjovas, D. Čygas, T. Andriejauskas, F. Tuminienė, Surface type and age effects on tyre/road noise levels, in: 10th Int. Conf. Environ. Eng. ICEE 2017, 2017. doi:10.3846/enviro.2017.152.

[18] B. Peeters, F. Reinink, W.J. Van Vliet, Close Proximity (CPX) Round Robin Test 2017, in: Euronoise 2018, Crete, 2018: pp. 2757–2764.

[19] P. Mioduszewski, W. Gardziejczyk, Inhomogeneity of low-noise wearing courses evaluated by tire/road noise measurements using the close-proximity method, Appl. Acoust. 111 (2016) 58–66. doi:10.1016/j.apacoust.2016.04.006.

[20] C. Vuye, A. Bergiers, B. Vanhooreweder, The Acoustical Durability of Thin Noise Reducing Asphalt Layers, Coatings. 6 (2016) 21. doi:10.3390/coatings6020021.

[21] H. Bendtsen, E. Kohler, Q. Lu, B. Rymer, California-Denmark study on acoustic aging of road pavements, Transp. Res. Rec. (2010) 122–128. doi:10.3141/2158-15.

[22] J. Kragh, B. Andersen, H. Bendtsen, Acoustical characteristics of Danish road surfaces - Danish Road Institute Technical note 38, 2006.

[23] L.G. Picado-Santos, S.D. Capitão, J.M.C. Neves, Crumb rubber asphalt mixtures: A literature review, Constr. Build. Mater. 247 (2020). doi:10.1016/j.conbuildmat.2020.118577.

[24] F. Guo, J. Zhang, J. Pei, B. Zhou, A.C. Falchetto, Z. Hu, Investigating the interaction behavior between asphalt binder and rubber in rubber asphalt by molecular dynamics simulation, Constr. Build. Mater. 252 (2020). doi:10.1016/j.conbuildmat.2020.118956.

[25] D.D. Carlson, M. Belshe, Rubberized AsphaltState of the TechnologyCapturing the Engineering Properties of Tire Rubber in Asphalt Pavements, (2010) 1–91.

[26] M.C. Zanetti, S. Fiore, B. Ruffino, E. Santagata, D. Dalmazzo, M. Lanotte, Characterization of crumb rubber from end-of-life tyres for paving applications, Waste Manag. 45 (2015) 161–170. doi:10.1016/j.wasman.2015.05.003.

[27] M. Losa, P. Leandri, G. Licitra, Mixture design optimization of low-noise pavements, Transp. Res. Rec. (2013) 25–33. doi:10.3141/2372-04.

[28] L. Teti, G. de León, A. Del Pizzo, A. Moro, F. Bianco, L. Fredianelli, G. Licitra, Modelling the acoustic performance of newly laid low-noise pavements, Constr. Build. Mater. 247 (2020) 118509. doi:10.1016/j.conbuildmat.2020.118509.

[29] P. Donavan, C. Janello, Arizona Quiet Pavement Pilot Program: Comprehensive Report SPR-577-2, Phoenix, Arizona, 2018.

[30] G. Licitra, A. Moro, L. Teti, A. Del Pizzo, F. Bianco, Modelling of acoustic ageing of rubberized pavements, Appl. Acoust. 146 (2019) 237–245. doi:10.1016/j.apacoust.2018.11.009.

[31] Q.Z. Wang, N.N. Wang, M.L. Tseng, Y.M. Huang, N.L. Li, Waste tire recycling assessment: Road application potential and carbon emissions reduction analysis of crumb rubber modified asphalt in China, J. Clean. Prod. 249 (2020). doi:10.1016/j.jclepro.2019.119411.

[32] T. Wang, F. Xiao, X. Zhu, B. Huang, J. Wang, S. Amirkhanian, Energy consumption and environmental impact of rubberized asphalt pavement, J. Clean. Prod. (2018). doi:10.1016/j.jclepro.2018.01.086.

[33] H. Bendtsen, B. Andersen, B. Kalman, J. Cesbron, The first poroelastic test section in PERSUADE, 42nd Int. Congr. Expo. Noise Control Eng. 2013, INTER-NOISE 2013 Noise Control Qual. Life. 1 (2013) 1–5.

[34] R. Stahlfest, H. Skov, H. Bendtsen, J. Cesbron, Laboratory measurements on poroelastic test slabs from full scale test sections, in: Euronoise 2015, 2020: pp. 1339–1344.

[35] H. Bendtsen, R.S.H. Skov, Performance of Eight PoroelasticTest Sections. Report nr. 547, 2015.

[36] M. Li, A.A.A. Molenaar, M.F.C. van de Ven, W. van Keulen, Mechanical Impedance Measurement on Thin Layer Surface With Impedance Hammer Device, J. Test. Eval. 40 (2012) 20120089. doi:10.1520/jte20120089.

[37] M. Li, W. Van Keulen, H. Ceylan, D. Cao, M. Van De Ven, A. Molenaar, Pavement stiffness measurements in relation to mechanical impedance, Constr. Build. Mater. 102 (2016) 455–461. doi:10.1016/j.conbuildmat.2015.10.191.

[38] F.G. Praticò, A. Moro, R. Ammendola, Factors Affecting Variance and Bias of Non-Nuclear Density

Gauges for Porous European Mixes and Densegraded Friction Courses, Balt. J. Road Bridg. Eng. 4 (2009) 99–107. doi:10.3846/1822-427X.2009.4.99-107.

[39] What is a Frequency Response Function (FRF)?, Siemens. (2019). https://community.sw.siemens.com/s/article/what-is-a-frequency-response-function-frf.

[40] EN 29052-1, Acoustics - Method for the determination of dynamic stiffness - Part 1: Materials used under floating floors in dwellings, 1992.

[41] ISO 7626-5, Mechanical vibration and shock — Experimental determination of mechanical mobility — Part 5: Measurements using impact excitation with an exciter which is not attached to the structure, 2019.

[42] ASTM C125, Standard Test Method for Fundamental Transverse, Longitudinal, and Torsional Resonant Frequencies of Concrete Specimens, 2002.

[43] EN 14146, Natural stone test methods - Determination of the dynamic modulus of elasticity (by measuring the fundamental resonance frequency), 2004.

[44] N. Bede, I. Kožar, Determination of Dynamic Modulus of Elasticity of Concrete by Impact Hammer, HDKBR INFO Mag. 6 (2016) 8–11.

[45] D. Thorby, Random Vibration, Struct. Dyn. Vib. Pract. (2008) 267–324. doi:10.1016/b978-0-7506-8002-8.00010-9.

[46] J. Wren, A Simple Frequency Response Function, Prosig Noise Vib. Blog. (2009). http://blog.prosig.com/2009/10/19/a-simple-frequency-response-function/.

[47] C.M. Harris, A.G. Piersol, Harris' shock and vibration handbook, (2002).

[48] V. Vicuña, DeterminationoftheDampingCoefficientUsingDifferentMaterialsonaSelectedSurface, (2016). doi:10.13140/RG.2.1.2313.6246.

[49] Siemens, How to calculate damping from a FRF?, (2019). https://community.sw.siemens.com/s/article/how-to-calculate-damping-from-a-frf.

[50] P. Bonfiglio, P. Fausti, Dynamic Stiffness Of Materials Used For Reduction In Impact Noise : Comparison Between Different Measurement Techniques, in: 2004.

[51] E. Uglova, A. Tiraturyan, Calculation of the Damping Factors of the Flexible Pavement Structure Courses According to the In-place Testing Data, Procedia Eng. 187 (2017) 742–748. doi:10.1016/j.proeng.2017.04.431.

[52] N. Hasheminejad, C. Vuye, W. Van Den Bergh, J. Dirckx, J. Leysen, S. Sels, S. Vanlanduit, Identification of pavement material properties using vibration measurements, in: Proc. ISMA 2016 - Int. Conf. Noise Vib. Eng. USD2016 - Int. Conf. Uncertain. Struct. Dyn., 2016: pp. 2217–2231.

[53] V.F. Vázquez, S.E. Paje, Mechanical impedance and CPX noise of SMA pavements Characteristics of the SMA mixtures, Acoust. 2012 Nantes Conf. (2012) 167–171.

[54] V.F. Vázquez, S.E. Paje, Dynamic Stiffness Assessment of Construction Materials by the Resonant and Non-resonant Methods, J. Nondestruct. Eval. 35 (2016) 1–11. doi:10.1007/s10921-016-0350-z.

[55] M. Radenberg, B. Drewes, R. Manke, Noise reducing effect of new dense asphalt layers, (2017). doi:10.14311/ee.2016.053.

[56] J. Kragh, L.M. Iversen, U. Sandberg, Nordtex Final Report Road Surface Texture for Low Noise and Low Rolling Resistance, 2013.

[57] F.G. Praticò, P.G. Briante, Prediction of surface texture for better performance of friction courses, Constr. Build. Mater. 230 (2020). doi:10.1016/j.conbuildmat.2019.116991.

[58] M. Duriez, J. Arrambide, Nouveau traité de matériaux de construction. Liants et bétons

hydrocarbonés, 2me ed., Dunod, Paris, 1962.

[59] C. Celauro, F.G. Praticò, Asphalt mixtures modified with basalt fibres for surface courses, Constr. Build. Mater. 170 (2018) 245–253. doi:10.1016/j.conbuildmat.2018.03.058.